

A Simple-but-effective Baseline for Training-free Class-Agnostic Counting

Yuhao Lin*, Haiming Xu*, Lingqiao Liu, Javen Qinfeng Shi
 Australian Institution for Machine Learning
 The University of Adelaide

yuhao.lin01, hai-ming.xu, lingqiao.liu, javen.shi@adelaide.edu.au

Abstract

Class-Agnostic Counting (CAC) seeks to accurately count objects in a given image with only a few reference examples. While previous methods achieving this relied on additional training, recent efforts have shown that it's possible to accomplish this without training by utilizing pre-existing foundation models, particularly the Segment Anything Model (SAM), for counting via instance-level segmentation. Although promising, current training-free methods still lag behind their training-based counterparts in terms of performance. In this research, we present a straightforward training-free solution that effectively bridges this performance gap, serving as a strong baseline. The primary contribution of our work lies in the discovery of four key technologies that can enhance performance. Specifically, we suggest employing a superpixel algorithm to generate more precise initial point prompts, utilizing an image encoder with richer semantic knowledge to replace the SAM encoder for representing candidate objects, and adopting a multiscale mechanism and a transductive prototype scheme to update the representation of reference examples. By combining these four technologies, our approach achieves significant improvements over existing training-free methods and delivers performance on par with training-based ones.

1. Introduction

Class-Agnostic Counting (CAC) [15] is increasingly gaining recognition in the field of computer vision. In contrast to traditional class-specific object counting [20, 23], which relies on training models for specific predefined categories, CAC adopts a more flexible approach. It expects the model to adapt to a diverse array of objects across various classes using only a minimal number of examples [15]. This adaptability makes CAC a compelling area of research, offering potential for broad application in scenarios where rapid or dynamic object recognition is required.

*Equally contributed.



Figure 1. Visualizing the performance, our method notably narrows the gap in counting accuracy between training-free and training-based approaches. Impressively, it even surpasses the top-performing training-based methods on the CARPK dataset, underscoring the potential of training-free approaches.

To attain the ability for Class-Agnostic Counting, a common approach is to utilize a training dataset containing various objects along with their corresponding density maps. This training data is used to train a model that compares visual features between reference examples and the query image [6, 15, 23]. This methodology enables class-independent adaptation, which is essential for scenarios requiring dynamic counting. However, a significant drawback of these methods is their reliance on large-scale annotated training data, which presents challenges in terms of labor intensity and scalability across diverse visual categories [17]. Recently, the Segment Anything Model (SAM) [10] has garnered substantial attention across various research domains due to its remarkable ability to generate high-quality object masks for any given image. This versatility has led to its application in numerous research areas, as evidenced by multiple studies [16, 22, 26, 28]. In the context of CAC, researchers have started adopting SAM for producing instance-level segmentation masks corresponding to referenced objects. By counting the number of instance masks, they can determine the final count of objects.

Thanks to SAM's robust instance segmentation capabil-

ities, this counting-via-instance-segmentation approach can function effectively even when utilizing the off-the-shelf SAM model without any additional training. Training-free methods hold appeal for CAC since they eliminate the need for a dedicated training dataset and alleviate the challenges associated with collecting extra training data. Nevertheless, despite their promise, current training-free CAC methods still lag behind their training-based counterparts in terms of performance, e.g., as demonstrated in Figure 1, the current top training-free method falls short of the best training-based approaches by 84.89% and 105.82% on the FSC-147 [20] and CARPK [9] datasets, respectively.

In our research, we introduce an improved approach to achieve training-free Class-Agnostic Counting using SAM. Our method provides a straightforward yet robust means to significantly narrow the performance gap often observed in training-free CAC methods. This positions our approach as a valuable benchmark for future research in this domain. Our approach to CAC relies on four pivotal technological components, each playing a crucial role: First, we emphasize the paramount importance of precise point prompt placement within SAM to achieve accurate object masking. To this end, we advocate the utilization of superpixels, which enables the creation of initial point prompts, resulting in high object recall without imposing significant computational overhead. Moreover, our thorough investigations have exposed limitations in SAM’s current image encoder concerning its ability to effectively capture semantic-level similarity. In response, we propose the adoption of image encoders equipped to capture richer semantic information. This proposition holds the potential to enhance the representation of objects during the counting process. Additionally, we recognize the significance of implementing a multiscale mechanism, particularly for the precise counting of small objects. By incorporating this mechanism, our approach accommodates variations in object size across diverse instances, thus yielding more accurate counting results. Finally, we introduce a transductive prototype update strategy for reference examples. Through the augmentation of reference examples with candidate objects that are likely to share the same object category, we substantially enhance the reference-candidate similarity metric. This enhancement empowers us to more effectively determine whether an object proposal qualifies as the target of interest, ultimately contributing to the overall accuracy of our Class-Agnostic Counting methodology. Collectively, these four technological advancements serve as the cornerstone of our approach.

Our rigorous experiments demonstrated the remarkable performance of our proposed methods and the effectiveness of the four key components. Significantly, we show for the first time that a Class-Agnostic Counting (CAC) model without any training can achieve performance on par with that of training-based CAC approaches.

2. Related Work

2.1. Class-Agnostic Counting Methods

Lu et al. [15] first address CAC, employed convolutional neural networks to extract and concatenate features from both query images and exemplars to estimate object counts. However, this method faced challenges related to overfitting when directly regressing from concatenated features. Addressing this, CFOCNet [30] introduced improvements by explicitly modeling similarity, using a Siamese network to track to improve localization and count accuracy.

Further enhancements in similarity modeling were proposed by Shi et al. [23] and You et al. [30], who integrated advanced techniques such as self-attention and learnable similarity metrics to reduce appearance variability and guide feature fusion, respectively. Moreover, the incorporation of a vision transformer for feature extraction by Liu et al. [13] marked a significant step towards leveraging the strengths of transformer models in the field, demonstrating the use of cross-attention to merge image and exemplar features effectively. Most recently, LOCA [6] introduces an object prototype extraction module that iteratively merges exemplar shape and appearance with image features, enabling adaptation from low-shot to zero-shot object counting scenarios.

However, these methods all need numerous training data, and the exemplar annotation is labor-consuming. In specific, the most commonly used dataset in CAC task, FSC-147 [20], includes 3659 training images with more than 10,000 exemplar annotations needed.

Ma et al. [17] first address CAC with Segment Anything Model (SAM) [10] in a training-free manner. After that Shi et al. [24] proposed a novel training-free object counter that introduces prior-guided mask generation to improve accuracy, along with a two-stage text-based object counting method, yielding competitive results on standard benchmarks. However, the performance of these training-free methods heavily lags behind the training-based CAC methods. In this work, we propose a simple but effective training-free approach to significantly reduce the performance gap.

2.2. Superpixel Methods

Superpixel is an important concept in computer vision, primarily used to group pixels into perceptually meaningful regions, which can significantly reduce the complexity of image processing tasks. As a way to effectively reduce the number of image primitives for subsequent processing, superpixel algorithms have been widely adopted in vision problems such as saliency detection [27], object detection [8], and semantic segmentation [25].

Superpixel was popularized by Ren and Malik [21] through their pioneering work on the Normalized Cuts al-

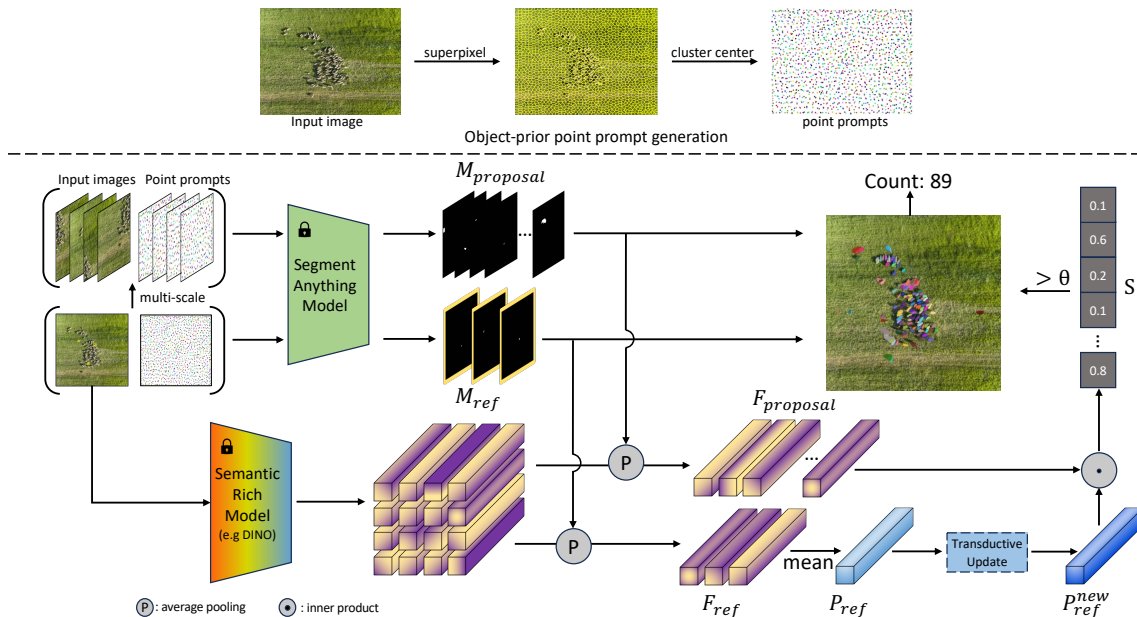


Figure 2. **Top** row illustrates the creation process of object-prior point prompts. **Bottom** row depicts a pipeline overview of our proposed training-free object counting approach. Details of the transductive update module are provided in Eq. 4. Reference objects are marked with yellow boxes in the input image (zoom in for clarity).

gorithm, and has been significantly advanced by the introduction of the Simple Linear Iterative Clustering (SLIC) [1] algorithm. SLIC uses K-means clustering in a five-dimensional space of color and pixel coordinates to create compact and uniform superpixels, which has made it a benchmark in the field. Several variants (LSC [12], Manifold SLIC [14], SNIC [2]) have been developed upon SLIC.

2.3. Vision Foundation Models

For pure vision area, DINO (self-Distillation with NO labels) [3] and its more advanced iteration, DINOv2 [18], represent significant strides in self-supervised learning within computer vision. Through a teacher-student distillation process that does not rely on labeled data, DINO masters semantic-rich visual representation. DINOv2 builds on this by refining the architecture and training mechanisms, further improving the model’s efficiency and the accuracy of learned representations.

Most recently, SAM [10] specializes in image segmentation, adeptly generating accurate object masks from prompts such as points and boxes. SAM’s proficiency is evidenced by its remarkable performance on diverse segmentation benchmarks and its zero-shot transfer abilities, which extend across a range of datasets [4, 5].

These foundation models collectively redefine the capabilities of computer vision systems. They provide a versatile framework for tackling new tasks and adapting to unfamiliar data distributions without the necessity of bespoke training [16, 26, 28].

3. Method

In this section, we introduce four innovative modules that enhance the effectiveness of employing SAM in training-free CAC, i.e., object-prior point prompt (Sec. 3.1) and semantic-rich feature (Sec. 3.2) are matters for the training-free model to deliver satisfactory counting outcomes. Additionally, the multi-scale strategy (Sec. 3.3) and transductive prototype updating (Sec. 3.4) help substantially elevate counting accuracy. The comprehensive framework of our method is depicted in Figure 2.

3.1. Object-prior Point Prompt Matters

In the use of SAM for zero-shot object proposal generation [10], a regular grid of point prompts is utilized to automatically generate class-agnostic masks. In the scenario of object counting, counted objects are usually tiny or crowded. In order to increase the recall of the object proposals, fine-grained grid point prompts became indispensable. As presented in Figure 3, naively increasing the number of points grid from 1600 to 3600 increases recall by 20%. However, an increase in the number of point grids leads to a doubling of computational time overhead. In order to ensure the recall rate without increasing time complexity too much, we propose to utilize the superpixel segmentation algorithm [21] to firstly perceptual group pixels into clusters and then take cluster centers as object-prior point prompts to feed into SAM for object proposal generation.

In this work, a superpixel algorithm named Simple Linear Iterative Clustering (SLIC) is used to generate compact

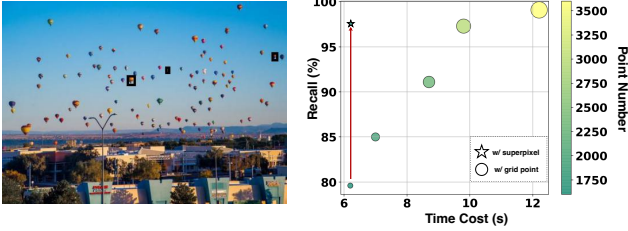


Figure 3. Effectiveness demonstration of the use of superpixel on the quality of mask proposals generated by SAM. **Left:** an image with reference exemplars (hot-air balloon) in black boxes. **Right:** a bubble chart illustrates the trade-off between the recall rate of the interested object and the time cost. Without increasing the number of point prompts, SAM with superpixel¹ can significantly improve the recall rate of hot-air balloons in the output mask proposals, thus avoiding the potential computational burden caused by the demand for denser point grids. Please find visualizations of the generated mask proposal in the appendix.

superpixels with a low computational overhead [1].

Given the initial cluster number K , SLIC can directly output superpixel centers $\mathcal{C} = \{(x_i, y_i)\}_{i=1}^K$. These centers, along with the provided reference boxes (or points) \mathcal{R} , can then be fed into SAM batch by batch for mask proposal generation

$$\mathcal{M}_{\text{ref}} = \mathbb{D}(\mathbb{E}(I), \mathcal{R}), \quad \mathcal{M}_{\text{proposal}} = \mathbb{D}(\mathbb{E}(I), \mathcal{C}) \quad (1)$$

where \mathbb{E} and \mathbb{D} are encoder and decoder of SAM respectively. I is the input image. \mathcal{M}_{ref} denotes the generated masks for corresponding referenced prompts (reference boxes or points) and $\mathcal{M}_{\text{proposal}}$ means all potential mask proposals².

3.2. Semantic-rich Feature Matters

When object masks are ready, the next step is to recognize all object masks similar to the given reference objects from $\mathcal{M}_{\text{proposal}}$. One straightforward way is to compare the similarity of the region-of-mask features (RoMF) of referenced objects to that of the RoMF of others

$$\begin{aligned} \mathcal{S}^i &= \text{sim}(\mathbf{P}_{\text{ref}}, F_{\text{proposal}}^i), \quad \text{where} \quad (2) \\ \mathbf{P}_{\text{ref}} &= \frac{1}{n_{\text{ref}}} \sum_{j=1}^{n_{\text{ref}}} \text{AvgPool}(\mathbb{E}(I), \mathcal{M}_{\text{ref}}^j) \\ F_{\text{proposal}}^i &= \text{AvgPool}(\mathbb{E}(I), \mathcal{M}_{\text{proposal}}^i) \end{aligned}$$

where AvgPool is the average pooling operation. n_{ref} is the number of given reference objects and is set to 3 by default

¹Performing superpixel on this example image takes only 10ms with AMD Ryzen 9 3900X CPU, a negligible computational expense compared to the SAM computation cost.

²The largest mask generated by SAM, which typically corresponds to the background, and masks for referenced objects are filtered from $\mathcal{M}_{\text{proposal}}$ for simplicity, i.e., $\mathcal{M}_{\text{proposal}} \cap \mathcal{M}_{\text{ref}} = \emptyset$.

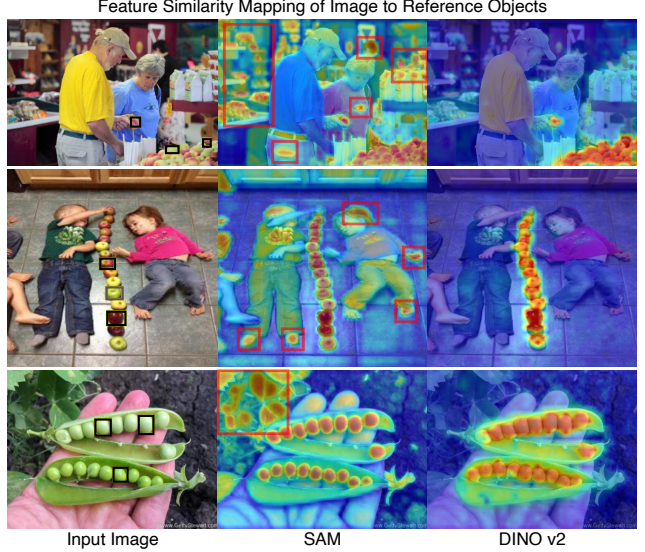


Figure 4. Visualization of the similarity mappings of image features to reference object features (marked in black boxes) using SAM and DINOv2. It distinctly shows that SAM’s similarity mapping erroneously highlights numerous areas unrelated to the target object, whereas DINOv2’s mapping accurately encompasses the objects of interest. This demonstrates that DINOv2’s features possess more semantically relevant knowledge.

in the literature [20]. \mathbf{P}_{ref} denotes the average of referenced object features, a.k.a prototypes. $\text{sim}(\cdot, \cdot)$ is the similarity function and the cosine function is used in this study. \mathcal{S}^i is the similarity score for each object proposal i .

Next, an overall segmentation for interested objects can be obtained by selecting mask proposals whose similarity score is higher than a predefined threshold θ . However, searching for an optimal θ can be hard due to the feature representations of SAM lacking clear semantic-related knowledge [11, 17]. As empirical analysis presented in Figure 4, many objects of different categories from the reference object may have a quite close similarity score to those objects of the same category, thus it is inevitable to output poor counting results with noisy segment generation. For instance, the SAM feature struggles to differentiate between apples and other messy objects in row 1, as well as children’s hair and feet in row 2 of Figure 4. Moreover, our empirical findings (the first two rows in Table 3) indicate that the enhanced recall of referenced objects achieved through the proposed superpixel method does not improve the final counting performance when the SAM feature representation is directly employed for object discrimination. Therefore, to obtain a plausible counting accuracy, using semantic-rich features for mask proposal selection becomes indispensable.

Recently, many vision foundation models with rich se-

³Multiple colors are used for the point grid in the figures of columns 2-4 for better visualization.

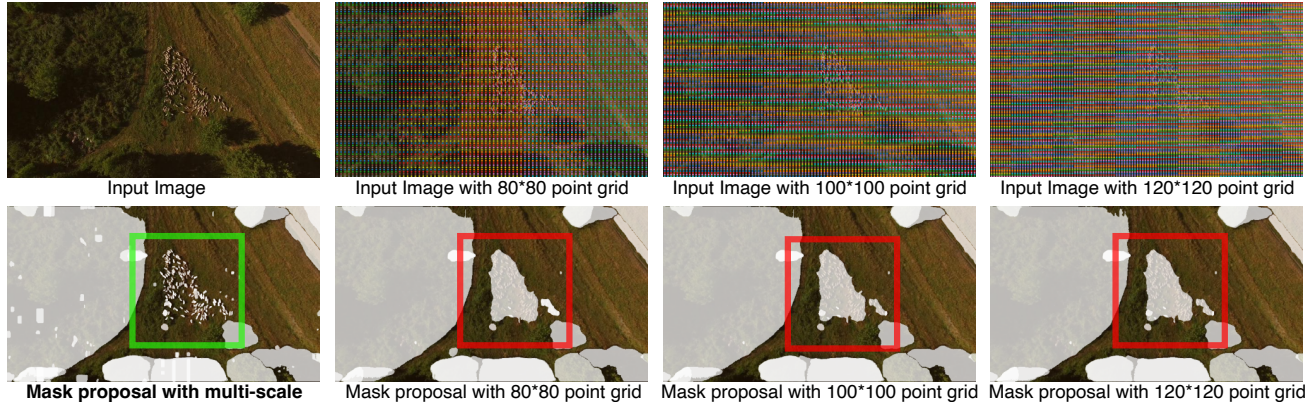


Figure 5. Effectiveness demonstration of our multi-scale mechanism in scenarios involving extremely tiny counting objects. Merely increasing the quantity of point prompts³ in SAM fails to yield accurate instance-level mask proposals. However, integrating SAM with our multi-scale mechanism (using 32*32 points for aerial photography of sheep in this demonstration) effectively achieves better mask quality.

mantic knowledge have been made accessible to the public, such as DINO [3, 18].

Combining with the semantic-rich feature representation, the final count can be obtained

$$\begin{aligned} \text{count} &= n_{\text{ref}} + \sum_{i=1}^N \mathbb{1}(\mathcal{S}^i > \theta), \quad \text{where} \quad (3) \\ \mathcal{S}^i &= \text{sim}(\mathbf{P}_{\text{ref}}, F_{\text{proposal}}^i), \\ \mathbf{P}_{\text{ref}} &= \frac{1}{n_{\text{ref}}} \sum_{j=1}^{n_{\text{ref}}} \text{AvgPool} \left(\mathbb{E}_{\text{sem}}(I), h(\mathcal{M}_{\text{ref}}^j) \right) \\ F_{\text{proposal}}^i &= \text{AvgPool} \left(\mathbb{E}_{\text{sem}}(I), h(\mathcal{M}_{\text{proposal}}^i) \right) \end{aligned}$$

where \mathbb{E}_{sem} is the encoder with rich semantic knowledge and $h(\cdot)$ is the interpolation function to accommodate the resolution of SAM generated mask to that of the encoder output. N is the number of object proposals. θ is the similarity threshold and is empirically set to 0.4 in this study.

3.3. Multi-scale Segmentation Helps

In the task of object counting, there exist some scenes where objects that need to be counted are extremely tiny and crowded, e.g., aerial photography of sheep. It becomes challenging for SAM to generate reasonable instance-level masks. As Figure 5 shows, naive increasing the number of points from 6400 to even 14400 still fails to make SAM generate precise mask proposals for the sheep instance. In order to tackle this problem, we propose a simple multi-scale mechanism. Specifically, we first cut the input image into $n_p \times n_p$ patches of the same size⁴. Then we resize these patches to the original size of the input image and feed them together with the original input image into SAM for mask proposal generation. Please see Figure 2 for details. As

⁴Empirically, $n_p = 2$ is found to perform well in this study.

the bottom left picture in Figure 5 shows, using this simple multi-scale mechanism can successfully obtain precise instance-level mask proposals.

3.4. Transductive Prototype Updating Helps

In Sec. 3.2, the prototype of the interested object \mathbf{P}_{ref} is simply the average of given few-shot reference object features. Since objects in the same class may have various appearances in the same image, this simple prototype may not be representative enough to match all interested objects. We argue that potentially interested-object features from mask proposals can be helpful for matching generalization and propose a novel transductive prototype updating strategy to improve the quality of the prototype

$$\mathbf{P}_{\text{ref}}^{\text{new}} = \frac{n_{\text{ref}} \cdot \mathbf{P}_{\text{ref}} + \sum_i^N \mathbb{1}(\mathcal{S}^i > \delta) \cdot F_{\text{proposal}}^i}{n_{\text{ref}} + \sum_i^N \mathbb{1}(\mathcal{S}^i > \delta)} \quad (4)$$

where δ is a similarity threshold and is set to 0.5 in this study for selecting plausible reference candidates.

4. Experiment

In this section, we first provide details of our experimental setup. Next, we assess our proposed method on two widely-used CAC benchmarks, comparing it against both training-based and training-free CAC methods. Lastly, we conduct comprehensive ablation studies to further explore the effectiveness of our approach.

4.1. Experimental Setup

Dataset: In our study, we assess our method using two popular datasets for counting tasks: FSC-147 [20] and CARPK [9]. FSC-147, the first extensive CAC dataset, includes 6,135 images across 147 categories, divided into 3,659 training, 1,286 validation, and 1,190 test images.

	Training	Reference Format	FSC-147		CARPK	
			MAE ↓	RMSE ↓	MAE ↓	RMSE ↓
GMN [15] [ACCV 19 [*]]	Yes	Box	26.52	124.57	9.90	-
FamNet [20] [CVPR 21 [*]]	Yes	Box	22.08	99.54	18.19	33.66
CFOCNet+ [29] [WACV 21 [*]]	Yes	Box	22.10	112.71	-	-
BMNet+ [23] [CVPR 22 [*]]	Yes	Box	14.62	91.83	5.76	7.83
SAFECount [30] [WACV 23 [*]]	Yes	Box	14.32	85.54	5.33	7.04
PseCo [7] [CVPR 24 [*]]	Yes	Box	13.05	112.86	-	-
LOCA [6] [ICCV 23 [*]]	Yes	Box	10.79	56.97	9.97	12.51
SAM Baseline [24]	No	N.A.	42.48	137.50	16.97	20.57
Count-Anything [17]	No	Box	27.97	131.24	-	-
TFOC [24] [WACV 24 [*]]	No	Box	19.95	132.16	10.97	14.24
Ours	No	Box	12.26	56.33	4.39	5.70
TFOC [24] [WACV 24 [*]]	No	Point	20.10	132.83	11.01	14.34
Ours	No	Point	12.47	49.97	4.39	5.70
TFOC [24] [WACV 24 [*]]	No	Text	24.79	137.15	-	-
Ours	No	Text	23.59	113.60	-	-

Table 1. Quantitative comparisons between our methods and others using point and box reference formats on the FSC-147 and CARPK benchmarks are presented. Our approach surpasses other training-free methods and shows competitive results against training-based ones. The best counting outcomes among training-free methods are emphasized in bold font.

Each image is annotated with bounding boxes and central points of three exemplars. Since our approach doesn’t require training, we focus solely on the test set, which features 1,190 images from 29 categories. The CARPK dataset comprises 1,448 images of car parks captured from drones. Following the protocol in [6, 23, 24], we select twelve exemplars from the training images of CARPK for use in all test images. Similar to FSC-147, our evaluation is confined to the test set, containing 459 images.

Evaluation Metrics: Follow [6, 23], we report the Mean Absolute Error (MAE), Root Mean Square Error (RMSE). In particular, $MAE = \frac{1}{n} \sum_{i=1}^n |y_i - \hat{y}_i|$, $RMSE = \sqrt{\frac{1}{n} \sum_{i=1}^n (y_i - \hat{y}_i)^2}$, where n is the number of test images, y is the ground truth and \hat{y} is the prediction.

Comparing Methods: Our approach is benchmarked against the latest state-of-the-art methods in both trained and training-free scenarios. For trained scenarios, we compare with several CAC techniques: GMN (General Matching Network [15]), FamNet (Few-shot adaptation and matching Network [20]), CFONet+ (Class-agnostic Few-shot Object Counting Network [29]), the advanced BMNet+ (Bilinear Matching Network [23]), SAFECount (similarity-aware feature enhancement [30]), and LOCA (Low-shot Object Counting network with iterative prototype Adaptation [6]). In the training-free setting, our models are evaluated alongside two existing methods: Count-Anything [17] and TFOC (training-free object counting [24]).

All experiments in this work are conducted on one NVIDIA GeForce RTX 3090 GPU and all other experimental settings (including the text prompt) are identical to the TFOC [24] approach for a fair comparison.

4.2. Comparison with State-of-the-Arts

Quantitative Results: Table 1 reports the comparison results on two popular CAC benchmarks. First, our approach achieves consistent performance improvements over the compared training-free methods on various evaluation metrics. Specifically, On the FSC-147 dataset, our approach lowers the Mean Absolute Error (MAE) to 12.26, outperforming the naive SAM Baseline, which has an MAE of 42.48, and the Count-Anything method with an MAE of 27.97. Compared to the state-of-the-art training-free method TFOC [24], the performance gain of our approach reaches **+7.69** MAE on the FSC-147 dataset and **+6.58** MAE on CARPK dataset. Meanwhile, the RMSE metric of our approach is also significantly lower than the TFOC method which demonstrates that our method can perform better in scenarios with more crowded objects.

Second, our approach greatly reduces the performance gap between the training-based and training-free methods. For example, on FSC-147, the gap has decreased from 9.16 to 1.47 on MAE and even outperformed 0.64 on RMSE. On the CARPK dataset, our approach excels in all the compared algorithms and creates a state-of-the-art performance.

Finally, we also evaluate the proposed method with point references and the consistent superior performance demonstrates the robustness of our approach.

We also evaluate our pipeline on FSC-147 test set with a one-shot counting scenario. Table 2 indicates that our approach is robust on a one-shot counting scenario, which is consistent with the results of the three-shot above.

And for text prompts, we followed TFOC [24] and employ the CLIP-Surgery model to derive coarse bounding

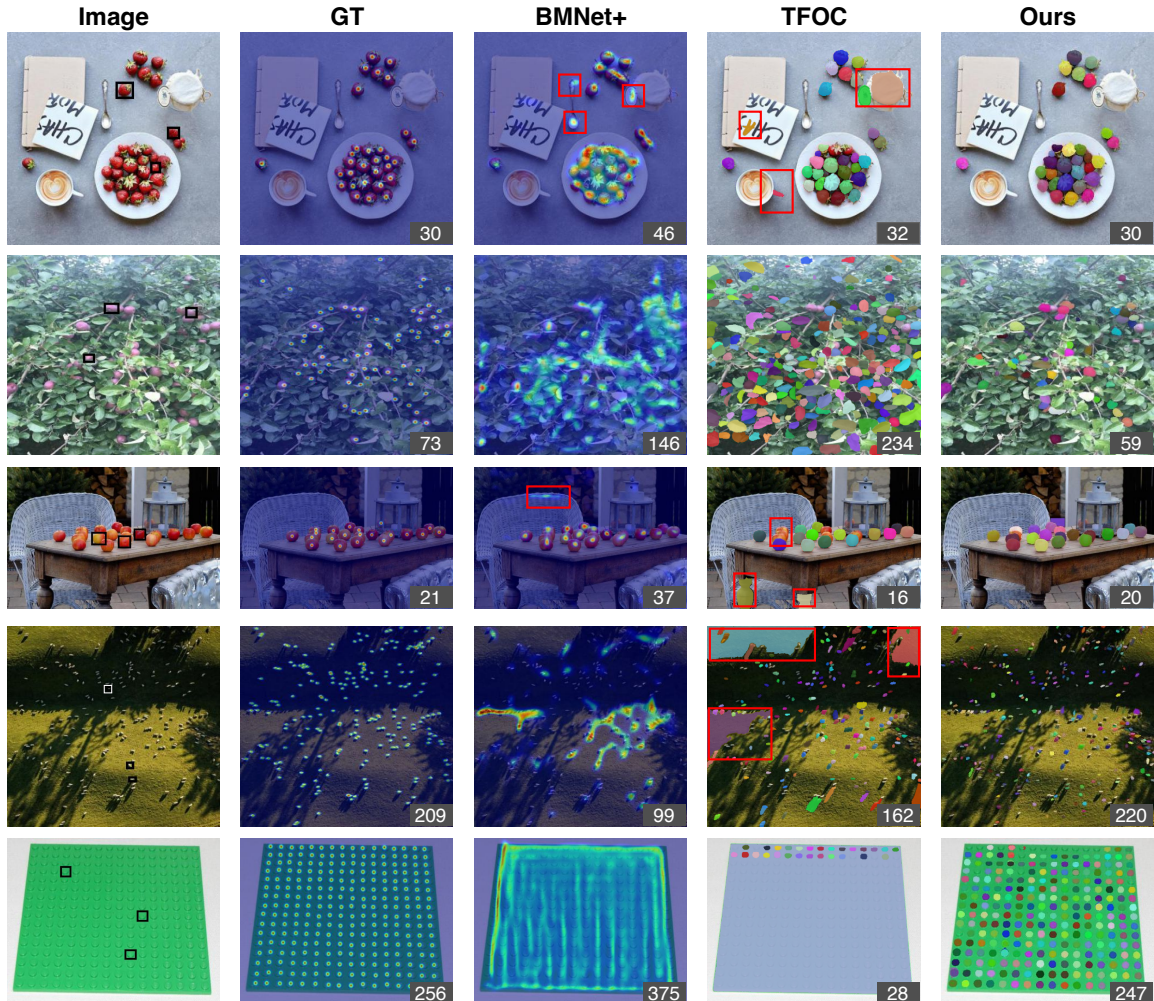


Figure 6. Qualitative results on the FSC-147 dataset are displayed. Exemplars are marked with black (white) boxes, and counting values are noted in the bottom-right corner. Error predictions are indicated by red boxes. Our method accurately predicts masks in both densely and sparsely populated scenes. Best viewed by zooming in.

	Training	FSC-147	
		MAE ↓	RMSE ↓
FamNet [20] [CVPR 21 [*]]	Yes	26.76	110.95
BMNet+ [23] [CVPR 22 [*]]	Yes	16.89	96.65
LOCA [6] [ICCV 23 [*]]	Yes	12.53	75.32
TFOC [24] [WACV 24 [*]]	No	22.96	137.27
Ours	No	15.15	69.16

Table 2. Evaluation on one-shot setting on FSC-147 test set.

boxes for the target object using text references. Then our approach use these coarse bounding boxes for object counting. As presented in last rows of the Table 1, our approach is slightly superior to the compared methods. The main reason is that the bounding boxes generated from TFOC [24] are not accurate. Technically, great improvement will be observed if high quality bounding boxes are given.

Qualitative Analysis: Figure 6 displayed the visualization results of various counting methods in different scenarios and our approach can always more accurately identify objects of interest in various scenes. Specifically, for scenes in the first three rows, both of the compared training-based and training-free methods mistakenly identified areas that do not belong to the interested object, such as the teacup handle and the spoon in row 1, the crowded leaves in row 2 and the table legs and the top edge of the chair back in row 3. While our approach can successfully and accurately segment out the interested object and produce a more accurate counting result. This will be attributed to the utilization of semantic-rich feature representations for SAM’s mask proposal selection in our approach. Furthermore, for more challenging scenes (the last two rows), the density maps generated by the training-based BMNet+ method are vague and exhibit substantial deviations in counting outcomes. The TFOC

Components				FSC-147	
SP	DINOv2	TPU	MS	MAE ↓	RMSE ↓
-	-	-	-	30.91	140.10
✓	-	-	-	30.89	140.06
-	✓	-	-	20.19	134.22
✓	✓	-	-	17.32	132.64
✓	✓	✓	-	16.04	132.40
✓	✓	-	✓	13.77	87.40
✓	✓	✓	✓	12.26	56.33

Table 3. Performance with different components on FSC-147. SP: superpixel, TPU: transductive prototype updating, MS: multi-scale.

number of K	MAE ↓	RMSE ↓	avg. time/image
50*50	5.09	6.66	5.26s
60*60	4.46	5.82	6.55s
64*64	4.39	5.70	7.04s

Table 4. Performance of our method with various K on CARPK.

method either erroneously includes extensive background areas in its object count or overlooks numerous objects in crowded scenes. Yet, our method yields accurate segmentation masks for individual objects due to its multi-scale mechanism, resulting in output counting numbers that more closely align with the ground truth.

5. Ablation study

In this section, we are interested in ablating our approach from the following perspective views on FSC-147 dataset:

Effectiveness of different components: Table 3 showcases the impact of each component in our method in both dataset. Specifically, although SAM with superpixel can achieve higher interested-object recall (shown in Figure 3), due to the lack of semantic differentiation ability in SAM features (shown in Figure 4), simply replacing default point grid with superpixel does not necessarily bring performance gains, as the results shown in the first two rows of Table 3. The next two rows show that using DINOv2 feature representation for SAM’s mask proposal selection significantly reduces the final counting error and the combing of superpixel can further bring performance gains. The subsequent two rows of Table 3 highlight the individual benefits of transductive prototype updating and the multi-scale mechanism on our model’s effectiveness. When these four components are combined, they lead to the most impressive counting results, especially in the RMSE metric..

Different number of initialized points: Table 4 shows that with 50*50 points, our method surpasses the previous SOTAs (see Table 1) in reasonable time. Increasing to 64*64 points further improves the MAE by 18%, while the computational time remains within seconds, demonstrating our method’s ability to achieve significant performance gains

SAM Backbone		MAE ↓	RMSE ↓
TFOC [24]	ViT-B	19.95	132.16
	ViT-H	30.41	138.28
Ours	ViT-B	14.43	87.54
	ViT-H	12.26	56.33

Table 5. Performance with different SAM backbone.

Vision Model	Patch Grid	MAE ↓	RMSE ↓
CLIP [19]	16*16	17.83	53.81
DINO [3]	28*28	14.28	59.33
DINO v2 [18]	37*37	12.26	56.33

Table 6. Performance with different semantic-rich model.

Update Round	MAE ↓	RMSE ↓
0	13.77	87.40
1	12.26	56.33
2	12.30	57.50

Table 7. Performance with various rounds of TPU.

with manageable time costs as the point density increases.

Backbone size of SAM: Table 5 compares TFOC and our method across different ViT backbones, revealing that our approach improves as the backbone scales from base to huge. In contrast, TFOC’s performance declines with ViT-H, possibly due to an increase in mask proposals leading to poorer selection. Our method, leveraging semantically rich features, benefits from the higher number of generated object proposals.

Various semantic-rich vision models: Table 6 displays our method’s performance across different SOTA foundation vision models, indicating that superior vision models yield improved counting accuracy. For CLIP, only the vision encoder is involved.

Multi-round transductive prototype updating: Our study typically employs one round of transductive prototype updating (TPU). Table 7 demonstrates that additional rounds do not enhance performance.

6. Conclusion

This paper presents a novel, training-free approach for Class-Agnostic Counting (CAC), significantly closing the performance gap with trained models. Key contributions include the use of superpixels, a richer semantic image encoder, a multiscale mechanism, and a transductive prototype updating strategy. Through rigorous experimental evaluation, the effectiveness of these four key components are demonstrated. The research shows that a CAC model without any training can achieve performance on par with training-based CAC approaches. This is a significant advancement in the field, indicating the potential of training-free approaches and setting a new benchmark for future research in CAC.

References

- [1] Radhakrishna Achanta, Appu Shaji, Kevin Smith, Aurelien Lucchi, Pascal Fua, and Sabine Süsstrunk. Slic superpixels compared to state-of-the-art superpixel methods. *IEEE transactions on pattern analysis and machine intelligence*, 34(11):2274–2282, 2012. **3, 4**
- [2] Radhakrishna Achanta and Sabine Süsstrunk. Superpixels and polygons using simple non-iterative clustering. In *Proceedings of the IEEE conference on computer vision and pattern recognition*, pages 4651–4660, 2017. **3**
- [3] Mathilde Caron, Hugo Touvron, Ishan Misra, Hervé Jégou, Julien Mairal, Piotr Bojanowski, and Armand Joulin. Emerging properties in self-supervised vision transformers. In *Proceedings of the IEEE/CVF international conference on computer vision*, pages 9650–9660, 2021. **3, 5, 8**
- [4] Xi Chen, Lianghua Huang, Yu Liu, Yujun Shen, Deli Zhao, and Hengshuang Zhao. Anydoor: Zero-shot object-level image customization. *arXiv preprint arXiv:2307.09481*, 2023. **3**
- [5] Ruining Deng, Can Cui, Quan Liu, Tianyuan Yao, Lucas W Remedios, Shunxing Bao, Bennett A Landman, Lee E Wheless, Lori A Coburn, Keith T Wilson, et al. Segment anything model (sam) for digital pathology: Assess zero-shot segmentation on whole slide imaging. *arXiv preprint arXiv:2304.04155*, 2023. **3**
- [6] Nikola Djukic, Alan Lukezic, Vitjan Zavrtnik, and Matej Kristan. A low-shot object counting network with iterative prototype adaptation. *arXiv preprint arXiv:2211.08217*, 2022. **1, 2, 6, 7**
- [7] Huang et al. Point segment and count: A generalized framework for object counting. In *CVPR*, 2024. **6**
- [8] Stephen Gould, Jim Rodgers, David Cohen, Gal Elidan, and Daphne Koller. Multi-class segmentation with relative location prior. *International journal of computer vision*, 80:300–316, 2008. **2**
- [9] Meng-Ru Hsieh, Yen-Liang Lin, and Winston H Hsu. Drone-based object counting by spatially regularized regional proposal network. In *Proceedings of the IEEE international conference on computer vision*, pages 4145–4153, 2017. **2, 5**
- [10] Alexander Kirillov, Eric Mintun, Nikhila Ravi, Hanzi Mao, Chloe Rolland, Laura Gustafson, Tete Xiao, Spencer Whitehead, Alexander C. Berg, Wan-Yen Lo, Piotr Dollár, and Ross Girshick. Segment anything. *arXiv:2304.02643*, 2023. **1, 2, 3**
- [11] Feng Li, Hao Zhang, Peize Sun, Xueyan Zou, Shilong Liu, Jianwei Yang, Chunyuan Li, Lei Zhang, and Jianfeng Gao. Semantic-sam: Segment and recognize anything at any granularity. *arXiv preprint arXiv:2307.04767*, 2023. **4**
- [12] Zhengqin Li and Jiansheng Chen. Superpixel segmentation using linear spectral clustering. In *Proceedings of the IEEE conference on computer vision and pattern recognition*, pages 1356–1363, 2015. **3**
- [13] Chang Liu, Yujie Zhong, Andrew Zisserman, and Weidi Xie. Countr: Transformer-based generalised visual counting. *arXiv preprint arXiv:2208.13721*, 2022. **2**
- [14] Yong-Jin Liu, Cheng-Chi Yu, Min-Jing Yu, and Ying He. Manifold slic: A fast method to compute content-sensitive superpixels. In *Proceedings of the IEEE conference on computer vision and pattern recognition*, pages 651–659, 2016. **3**
- [15] Erika Lu, Weidi Xie, and Andrew Zisserman. Class-agnostic counting. In *Computer Vision—ACCV 2018: 14th Asian Conference on Computer Vision, Perth, Australia, December 2–6, 2018, Revised Selected Papers, Part III 14*, pages 669–684. Springer, 2019. **1, 2, 6**
- [16] Jun Ma and Bo Wang. Segment anything in medical images. *arXiv preprint arXiv:2304.12306*, 2023. **1, 3**
- [17] Zhiheng Ma, Xiaopeng Hong, and Qinnan Shanguan. Can sam count anything? an empirical study on sam counting. *arXiv preprint arXiv:2304.10817*, 2023. **1, 2, 4, 6**
- [18] Maxime Oquab, Timothée Darcet, Théo Moutakanni, Huy Vo, Marc Szafraniec, Vasil Khalidov, Pierre Fernandez, Daniel Haziza, Francisco Massa, Alaaeldin El-Nouby, et al. Dinov2: Learning robust visual features without supervision. *arXiv preprint arXiv:2304.07193*, 2023. **3, 5, 8**
- [19] Alec Radford, Jong Wook Kim, Chris Hallacy, Aditya Ramesh, Gabriel Goh, Sandhini Agarwal, Girish Sastry, Amanda Askell, Pamela Mishkin, Jack Clark, et al. Learning transferable visual models from natural language supervision. In *International conference on machine learning*, pages 8748–8763. PMLR, 2021. **8**
- [20] Viresh Ranjan, Udbhav Sharma, Thu Nguyen, and Minh Hoai. Learning to count everything. In *CVPR*, pages 3394–3403, 2021. **1, 2, 4, 5, 6, 7**
- [21] Ren and Malik. Learning a classification model for segmentation. In *Proceedings ninth IEEE international conference on computer vision*, pages 10–17. IEEE, 2003. **2, 3**
- [22] Qihong Shen, Xingyi Yang, and Xinchao Wang. Anything-3d: Towards single-view anything reconstruction in the wild. *arXiv preprint arXiv:2304.10261*, 2023. **1**
- [23] Min Shi, Hao Lu, Chen Feng, Chengxin Liu, and Zhiguo Cao. Represent, compare, and learn: A similarity-aware framework for class-agnostic counting. In *Proceedings of the IEEE/CVF Conference on Computer Vision and Pattern Recognition*, pages 9529–9538, 2022. **1, 2, 6, 7**
- [24] Zenglin Shi, Ying Sun, and Mengmi Zhang. Training-free object counting with prompts. *arXiv preprint arXiv:2307.00038*, 2023. **2, 6, 7, 8**
- [25] Guang Shu, Afshin Dehghan, and Mubarak Shah. Improving an object detector and extracting regions using superpixels. In *Proceedings of the IEEE Conference on Computer Vision and Pattern Recognition*, pages 3721–3727, 2013. **2**
- [26] Teng Wang, Jinrui Zhang, Junjie Fei, Yixiao Ge, Hao Zheng, Yunlong Tang, Zhe Li, Mingqi Gao, Shanshan Zhao, Ying Shan, et al. Caption anything: Interactive image description with diverse multimodal controls. *arXiv preprint arXiv:2305.02677*, 2023. **1, 3**
- [27] Chuan Yang, Lihe Zhang, Huchuan Lu, Xiang Ruan, and Ming-Hsuan Yang. Saliency detection via graph-based manifold ranking. In *Proceedings of the IEEE conference on computer vision and pattern recognition*, pages 3166–3173, 2013. **2**

- [28] Jinyu Yang, Mingqi Gao, Zhe Li, Shang Gao, Fangjing Wang, and Feng Zheng. Track anything: Segment anything meets videos. *arXiv preprint arXiv:2304.11968*, 2023. [1](#), [3](#)
- [29] Shuo-Diao Yang, Hung-Ting Su, Winston H Hsu, and Wen-Chin Chen. Class-agnostic few-shot object counting. In *Proceedings of the IEEE/CVF Winter Conference on Applications of Computer Vision*, pages 870–878, 2021. [6](#)
- [30] Zhiyuan You, Kai Yang, Wenhan Luo, Xin Lu, Lei Cui, and Xinyi Le. Few-shot object counting with similarity-aware feature enhancement. In *Proceedings of the IEEE/CVF Winter Conference on Applications of Computer Vision*, pages 6315–6324, 2023. [2](#), [6](#)